

# On Designing Biopolymer-Bound Soil Composites (BSC) for Peak Compressive Strength

Isamar Rosa<sup>1</sup>, Henning Roedel<sup>1</sup>, Maria I. Allende<sup>1</sup>, Michael D. Lepech<sup>1,\*</sup> and David J. Loftus<sup>2</sup>

<sup>1</sup>Department of Civil and Environmental Engineering, Stanford University, Stanford, CA 94305, USA

<sup>2</sup>Division of Space Biosciences, NASA Ames Research Center, Moffet Field, CA 94035, USA

\*Corresponding Author: Michael D. Lepech. Email: mlepech@stanford.edu

Received: 21 January 2020; Accepted: 13 May 2020

**Abstract:** Biopolymer-bound Soil Composites (BSC), are a novel bio-based construction material class, produced through the mixture and desiccation of biopolymers with inorganic aggregates with applications in soil stabilization, brick creation and *in situ* construction on Earth and space. This paper introduces a mixture design methodology to produce maximum strength for a given soil-biopolymer combination. Twenty protein and sand mix designs were investigated, with varying amounts of biopolymer solution and compaction regimes during manufacture. The ultimate compressive strength, density, and shrinkage of BSC samples are reported. It is observed that the compressive strength of BSC materials increases proportional to tighter particle packing (soil dry bulk density) and binder content. A theory to explain this peak compressive strength phenomenon is presented.

**Keywords:** Compressive strength; biopolymer composites; material design; soil bulk density; in situ material utilization; sustainable materials

## 1 Introduction

Ordinary Portland Cement Concrete (OPCC) is the most consumed man-made material globally, due in part to its versatility and low cost. However, the manufacture of OPCC accounts for 5% of global anthropogenic CO<sub>2</sub> emissions, and much of the material used in its makeup comes from non-renewable sources [1,2]. Thus, new construction materials and methods that are vastly different from current practice, and utilize local, renewable resources are needed. Recognizing the potentially low impact of biological materials used in construction, a renewable and reusable protein biopolymer is studied in this work as a novel binder for granular soils and other aggregates. This biopolymer strategy stems from NASA's effort to develop closed loop building material systems for extraterrestrial environments [3].

Biopolymer-bound Soil Composites, or BSC, are a mixture of granular soil aggregate, biopolymer, and water, which is then desiccated to form a solid composite. During the manufacturing process, BSC transforms from a 'green', or wet, state to a stronger and stiffer state through the evaporation of water. In this work the main biopolymer used is the protein *bovine serum albumin* (BSA), which is dissolvable in water. Hence the material after its functional lifetime can be dissolved back into its main components to be remanufactured.



This work is licensed under a Creative Commons Attribution 4.0 International License, which permits unrestricted use, distribution, and reproduction in any medium, provided the original work is properly cited.

In addition to BSC materials studied in this paper, other research efforts have independently created alternate biopolymer-bound soil composites for a myriad of construction applications. Tab. 1 summarizes recent work on binding soils with biopolymers that can also be classified as BSC by highlighting the application, biopolymer binder used and resulting compressive strength. The work presented in this paper presents a methodology to more broadly aid in the material design of BSC materials to achieve maximum compressive strength.

**Table 1:** Summary of recent works exploring biopolymer soil composites (BSC). Soil types given in parentheses are based on the Unified Soil Classification System

Application	Biopolymer binder	Soil type	$M_c$	$\%w_{BP/S}$	Bulk Density ( $g/cm^3$ )	Comp. Strength (MPa)	Source
Soil Improvement	Agar with starches (Staramic 105 and 747, Starpol 136, 469, 600 and 700) (polysaccharides)	Fontainebleau sand (SP)	~30%	0.3–1.2%	1.50–1.54	0.12–0.5	Khatami et al. [4]
	Beta-1,3/1,6-glucan (polysaccharide)	Korean residual soil–KRS (CL)	60%	0.005–0.5%	N/A	1.0–4.3	Chang et al. [5]
	Xanthan gum (polysaccharide)	Sand (SP)	29%	0.5–1.5%	1.43–1.47	0.3–1.2	Chang et al. [6]
		In-situ Soil (SP-SM)	29%		1.74–1.63	3.0–4.2	
		KRS (CL)	60%		1.5–1.41	4.1–5.4	
	Xanthan gum, Gellan gum, Starpol 136 (polysaccharides)	Clay (CH)	60%		1.31	2.5	
Sand (SP)		10–15%	0.03–0.3%	1.97–2.07	0.06–0.49	Ayeldeen et al. [7]	
Silt (MH)			1.58–1.74	0.06–0.84			
Bricks	Xanthan gum (polysaccharide)	Sand (SP)	12–15%	1–5%	1.63–1.67	0.7–1.7	Qureshi et al. [8]
	Alginates (polysaccharides with salts)	Three types of clay (CL)	15–16%	0.1–0.5%	1.8–2.1	0.8–3.0	Dove et al. [9]
Construction Material	Xanthan gum, Gellan gum (polysaccharides)	Korean residual soil (CL)	60%	1%	1.34–1.37	2.5–6.5	Chang et al. [10]
	Guar gum, Xanthan gum (polysaccharides)	Soil Mixture (SC or SM)	10–13%	0.5–3%	~2.0	1.5–4.5 2.0–4.8	Muguda et al. [11]
	Animal Plasma AP920 (Proteins)	#90 Grade Sand (SP)	9–27%	6–18%	1.2–1.5	3.6–22.7	This paper

In the case of BSC bound by proteins, the binder increases in strength and stiffness through desiccation due to a glass-like arrest of the protein molecules at high concentration [12]. Hence the desiccated protein phase in BSC acts as a binder for the aggregate particles, providing resistance to translation and rotation that are typical of granular material flows, resulting in rigidity and strength of the composite. Additional descriptions of mechanical and microstructure characterizations of BSC materials can be found in [13–15].

For mass-produced construction materials, like OPCC and Asphalt Concrete (AC), many studies have related the design of these mixtures to targeted material properties, such as compressive strength, permeability, density, thermal conductivity, and environmental impact [16–18]. For each mixture design

methodology, there are key metric of material composition that relate directly to desired material properties. These metrics form the basis of a material design and engineering rationale.

For OPCC mixture design, which focuses on achieving a targeted compressive strength, it has long been understood that the water-to-cement (w/c) ratio is a key design metric. Lower values of water-to-cement ratio lead to higher compressive strength, but lower mixture workability. Studies of the water-to-cement ratio have shown that the ratio can go lower than 0.1 with the use of superplasticizers [19]. Normal mixtures without additives, however, require a minimum water-to-cement ratio of approximately 0.4 for workability [16]. For Asphalt Concrete (AC) materials, the amount of binder, measured as the voids filled with asphalt (VFA), the voids in mineral aggregate (VMA), and air voids, are three important measures that are used to design a high quality AC mixture [17]. Based on the Superpave standard by the Strategic Highway Research Program used in current AC mix design, VMA values should range between 11% and 15%, and VFA values from 65–80%. The optimal amount of binder is achieved when air voids are approximately 4% after compaction, which historically has been chosen to allow for additional compaction from traffic loads, and to prevent performance degradation when the void content becomes zero [20,21]. Both OPCC and AC mixture design methodologies also specify aggregate characteristics, such as particle size, shape, and angularity, as important characteristics for the successful design of compressive strength of the mixtures [22].

Recognizing that a rational method is needed to engineer the mechanical properties of BSC material, and promote further study, this paper presents a mixture design theory for achieving peak compressive strength of BSCs. Twenty mix designs with varying component proportions and compaction regimens were studied for an experimental soil (sand) and biopolymer binder (dried blood plasma proteins). The mixture design theory is based on a fundamental understanding of the mechanics of the material as they relate to the primary constituents of the desiccated composite–biopolymer solution and soil. Experimental results from more than 150 uniaxial compression tests and 20 shrinkage investigations of BSC with varying amounts of protein binder are presented. It was found that the soil bulk density, biopolymer content, and biopolymer saturation ratio have the largest effects on the composite peak compressive strength and are important mixture design variables.

## 2 Mixture Design Theory

As manufactured, BSC consists of densely packed soil particles with a biopolymer binder partially filling the void spaces between the particles (Fig. 1). It is hypothesized that BSC's compressive strength is largely a result of the soil particles bearing the majority of the load, with the biopolymer matrix providing the particles with shear resistance [23]. Hence, the goal of designing BSC mixtures with maximum compressive strength is to achieve a maximum dry soil bulk density, while also introducing as much biopolymer binder into the voids as possible. A methodology to balance these two efforts is shown in Tab. 2 and is discussed step by step.

### *Step 1: Find the Maximum Biopolymer Solution Concentration*

Similar to OPCC mixture design theory, one key consideration is workability of the fresh material. BSC material is produced by dissolving biopolymer into an aqueous solution, and then mixing this aqueous solution with soil. However, there exists an upper limit to the amount of biopolymer that can exist in solution before the solution viscosity changes dramatically as it undergoes glass-like kinetic arrest. Brownsey et al. [12] found this maximum mass concentration, referred here as  $(\% w/w_{BP})_{max}$ , to be 55% for bovine serum albumin. Experimentally, mix with such high biopolymer concentration are hard to manufacture with current methods, hence a value of 48% was used as the maximum. Biopolymer solution concentration is a key design variable for BSC and is defined in Eq. (1).

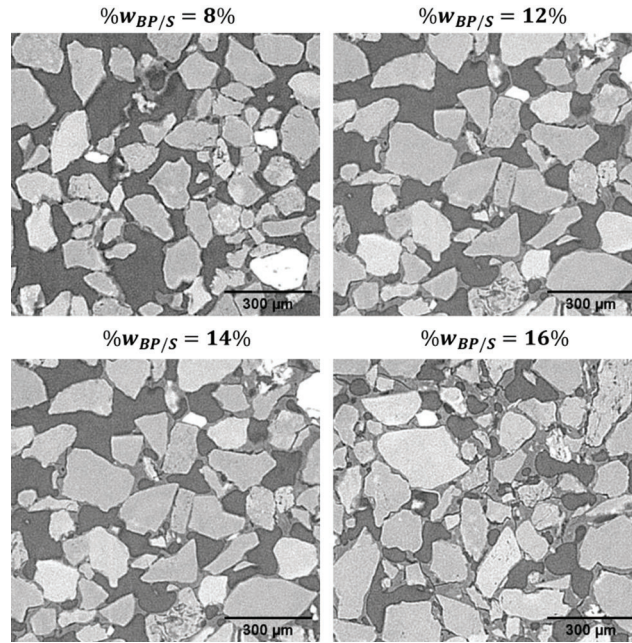


**Figure 1:** Microstructure of BSC at varying biopolymer to soil ratios  $\%w_{BP/S}$  captured using X-ray Microcomputed Tomography ( $\mu$ CT) (after [15]). The mixes correspond to mix 16 ( $\%w_{BP/S} = 8\%$ ), mix 17 ( $\%w_{BP/S} = 12\%$ ), mix 19 ( $\%w_{BP/S} = 14\%$ ), and mix 14 ( $\%w_{BP/S} = 16\%$ ) in Tab. 3

**Table 2:** Methodology for designing Biopolymer-bound Soil Composites (BSC) for maximum strength. Values are shown for the soil-biopolymer combination used in this study (sand and dried blood plasma)

Step	Equation and Value	Source
1. Determine the maximum biopolymer concentration $(\%w/w_{BP})_{max}$ in solution	Eq. (1) $(\%w/w_{BP})_{max} = 48\%$	Literature or experiments
2. Find the density of the biopolymer solution $\rho_{BP\ sol.}$ at the maximum biopolymer concentration	Eq. (2) $\rho_{BP\ sol.}(48\%) = 1.15\text{ g/cm}^3$	Literature or experiments
3. Specify the volume of BSC material desired	$V_{mix}$	
4. Find the maximum dry bulk density $\rho_{dry,bulk\ soil}^{max}$ for the particular soil and manufacturing method to be used	$\rho_{dry,bulk\ soil}^{max} = 1.48\text{ g/cm}^3$	Experiments
5. Determine the density of the soil particles $\rho_{soil}$	$\rho_{soil} = 2.6\text{ g/cm}^3$	Literature or experiments
6. Calculate the amount of soil needed to manufacture the desired volume of BSC	Eq. (3) $m_{soil}$	
7. Calculate the minimum volume fraction of voids $V_v^{min}$	Eq. (4) $V_v^{min} = 0.43$	
8. Calculate the mass of biopolymer solution required to manufacture the desired volume of BSC	Eq. (6) $m_{BP\ Sol.}$	
9. Calculate the mass of biopolymer and mass of water required to manufacture the desired volume of BSC	Eq. (7) $m_{BP}$ Eq. (8) $m_w$	

$$(\%w/w_{BP}) = \frac{m_{BP}}{m_{BP} + m_{water}} = \frac{m_{BP}}{m_{BP Sol.}} \quad (1)$$

where  $m_{BP Sol.}$  is the mass of the solution and is equal to the dry mass of the biopolymer  $m_{BP}$  plus the mass of water  $m_{water}$ . For other biopolymers, the method used by Brownsey et al. can be used to determine the maximum mass concentration of a biopolymer solution [12].

*Step 2: Calculate the Density of Biopolymer Solution at the Maximum Concentration*

Biopolymer solution density changes with biopolymer solution concentration due to the volume of solution effect. Using the method of partial specific volume and data for BSA from Bernhardt and Pauly [24], the density of the biopolymer solution for any given gravimetric concentration of BSA,  $\%w/w_{BP}$  can be estimated using Eq. (2).

$$\rho_{BP sol.} = \frac{1}{\sum m_i \bar{v}_i} = \frac{1}{\% (w/w)_{BP} * 0.734 \text{ cm}^3/\text{g} + (1 - \% (w/w)_{BP}) * 1.003 \text{ cm}^3/\text{g}} \quad (2)$$

where,  $\rho_{BP sol.}$  is the biopolymer solution density,  $\bar{v}_i$  is the partial specific gravity of the component,  $m_i$  is the mass fraction of the component and the temperature of water and the solution is taken to be 25°C. Although Bernhardt and Pauly data is up to 36% concentration, the theory can be extended to higher concentration to obtain an acceptable estimate for the purpose of mix design. Additionally, although blood plasma is composed of other proteins in addition to BSA, globulins, another main component, are non-conjugated proteins whose partial specific volume is clustered at 0.735 cm<sup>3</sup>/g, very close to the BSA values. Values for partial specific volumes can be found in the literature for other biopolymers in solution, or experimentally determined following the methods of Bernhardt and Pauly and Durchschlag [24,25].

*Step 3: Specify the Volume of BSC Material Desired*

*Step 4: Find Maximum Dry Bulk Density for Soil and Manufacturing Method*

Similar to both OPCC and AC materials, greater fractions of soil or aggregate per unit volume of material increase the peak compressive strength of BSC. This relationship is responsible for particle packing algorithms used to optimize aggregate gradations in OPCC and AC [26–29].

In the case of soil materials, the maximum bulk density of the soil fraction is influenced by the compaction methods and the soil moisture content [30]. Thus, the maximum dry soil bulk density,  $\rho_{dry,bulk soil}^{max}$ , is experimentally determined using a modified ASTM Standard C29 method and adopting the same compaction protocols as intended for final manufacturing [31].

*Step 5: Determine the Density of the Soil Particles*

The density of the soil particles can be found from product specifications, in literature, or through laboratory experiments (i.e., ASTM D854).

*Step 6: Calculate the Mass of Soil Required to Manufacture the Desired Volume of BSC*

It is assumed that the composite will reach maximum bulk density in order to achieve peak compressive strength. Thus, the mass of soil needed for manufacturing a desired volume of BSC can be estimated using Eq. (3) and assuming that the wet bulk soil density is approximately equal to the dry bulk soil density. This assumption is reasonable when the saturation ratio does not exceed unity, as will be discussed in Step 7.

$$m_{soil} = \rho_{dry,bulk soil}^{max} \times V_{mix} \quad (3)$$

*Step 7: Calculate the Minimum Volume Fraction of Voids*

The volume of biopolymer solution,  $V_{BS\ Sol.}$ , must not exceed the available void volume,  $V_v$ , at the maximum bulk density (i.e., the minimum void fraction  $V_v^{min}$ ) or the voids between the soil particles in BSC will become oversaturated. Thus, a crucial step in designing BSC for peak compressive strength is calculating this minimum void fraction ( $V_v^{min}$ ) using Eq. (4).

$$V_v^{min} = 1 - \frac{\rho_{dry,bulk\ soil}^{max}}{\rho_{soil}} \quad (4)$$

where  $\rho_{soil}$  is the density of the soil particles.

*Step 8: Calculate the Mass of Biopolymer Solution Required to Manufacture the Desired Volume*

The volume fraction of solution,  $V_{BP\ sol.}$ , can be calculated such that  $V_{BS\ Sol.} \leq V_v^{min}$ , or the Biopolymer Saturation Ratio  $V_{BP\ Sol.}/V_v^{min}$  must be less than or equal to unity (Eq. (5)). This limit is imposed since a saturation ratio greater than 1.0 will produce lower strength BSC materials due to larger pores and shrinkage cracks in the biopolymer phase.

$$\frac{V_{BP\ Sol.}}{V_v^{min}} \leq 1.0 \quad (5)$$

Thus, to maximize the amount of biopolymer binder, a biopolymer saturation ratio of unity is used to calculate the mass of biopolymer solution needed, following Eq. (6).

$$m_{BP\ sol.} = \rho_{BP\ sol.} V_v^{min} V_{mix} \quad (6)$$

where  $V_{mix}$  is the total volume of the fresh BSC mix taken from Step 3.

*Step 9: Calculate the Mass of Biopolymer and the Mass of Water Required to Manufacture the Desired Volume of BSC*

Using the maximum biopolymer solution concentration identified in Step 1 and the mass of biopolymer solution calculated in Step 8, the mass of biopolymer and mass of water required to manufacture the desired volume of BSC can be calculated using Eqs. (7) and (8), respectively, which are derived from Eq. (1). In the case of biopolymers with a moisture content greater than 0, the equations should be modified to account for the additional water.

$$m_{BP} = (\%w/w_{BP})_{max} * m_{BP\ sol.} \quad (7)$$

$$m_w = m_{BP\ sol.} - m_{BP} \quad (8)$$

In addition to the steps previously described, two other important descriptors of BSC mixtures are the biopolymer to soil mass ratio,  $\%w_{BP/S}$ , and the moisture content,  $M_c$ , defined as the mass ratio of water to soil.  $\%w_{BP/S}$  is useful for describing dry mixes of BSC because it indicates the ratio of biopolymer binder to soil particles when BSC materials are fully desiccated after manufacture. Using the mixture design methodology detailed above, the maximum  $\%w_{BP/S}$  for a given biopolymer-bound soil material can be calculated. For the soil and biopolymer combination experimentally studied in this paper,  $\%w_{BP/S}$  is equal to 18.7% assuming a maximum concentration  $(\%w/w_{BP})_{max}$  of 55% (from Step 2) and a maximum soil dry bulk density  $\rho_{dry,bulk\ soil}^{max}$  of 1.48 g/cm<sup>3</sup> from (Step 4).

As mentioned previously, the goal of designing BSC mixtures with maximum compressive strength is to achieve a maximum dry soil bulk density while also introducing as much biopolymer binder into the voids as possible. Using dry soil bulk density,  $\rho_{dry,bulk\ soil}$ , and the biopolymer to soil mass ratio,  $\%w_{BP/S}$ , BSC material design space for possible mixture combinations can be created, and is shown in Fig. 2. As seen in Fig. 2, there is a large solution space that is “efficient and feasible.” These are mixture designs that have dry soil bulk densities that are below the maximum value determined in Step 4 of the mixture

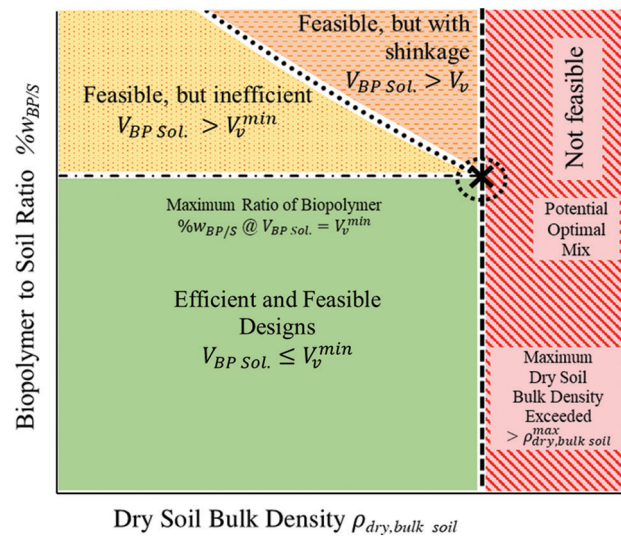


**Figure 2:** Design space for biopolymer-bound soil composite mixtures

design methodology (Tab. 2), and biopolymer to soil ratios for which the volume of biopolymer solution is equal to the volume of voids, up to the maximum concentration of biopolymer in solution,  $(\%w/w_{BP})_{max}$ . Mixtures that contain a volume of biopolymer solution greater than the volume of voids are deemed “feasible, but inefficient”, since too much biopolymer solution has been introduced into the mixture. As the dry bulk density of the mixture approaches the maximum, this “feasible, but inefficient” design space changes to “feasible, with shrinkage”, indicating a higher likelihood for the formation of shrinkage cracks during desiccation. These shrinkage cracks can lead to lower compressive strength of the composite. The design space is marked “not feasible” at dry bulk densities above the maximum determined in Step 4 of the mixture design methodology (Tab. 2). The BSC mixture with peak compressive strength, as designed according to the methodology presented in Tab. 2, maximizes both the dry soil bulk density and the biopolymer to soil mass ratio, shown in Fig. 2 with an “X” mark.

### 3 Materials and Experimental Methods

#### 3.1 Experimental Design

Sand (small particle sized feldspathic amber glass) was used as the inorganic aggregate for this experimental study. The sand was purchased from P.W. Gillibrand, Simi Valley, California, USA with trade name #90 Silver Sand [32]. The sand’s particle density,  $\rho_{soil}$ , is reported by the manufacturer as  $2.6 \text{ g/cm}^3$ . Fifteen independent measurements of the sand’s maximum dry bulk density  $\rho_{dry,bulk soil}^{max}$  were made following a modified ASTM Standard C29 protocol [31]. Sand samples were compressed to 10 MPa. The bulk density of the sand under these laboratory conditions was  $1.48 \text{ g/cm}^3 \pm 0.04 \text{ g/cm}^3$ .

Bovine blood plasma proteins were used in the manufacture of BSC specimens. This preparation of proteins primarily consists of albumin and immunoglobins, sold under the tradename *AP920 Bovine Plasma*, and purchased from APC, Inc. (Ankeny, IA). The biopolymer was used as received from the manufacturer. This biopolymer binder was chosen due to its lower environmental footprint and similar mechanical properties, when compared to purified *bovine serum albumin*, and also its availability in bulk quantities [33]. AP920 contains (by mass) 78% protein, 10% ash, 8% water, with fiber, lipids, and minerals making up the remaining fraction [34]. Of the protein fraction, AP920 contains 50–60% albumins, 40–50% globulins, and 1–3% fibrinogen [35]. The biopolymer water content was measured in

**Table 3:** Experimental mixture designs of biopolymer-bound soil composites

Mix Name	Mix Components (% mass)			$\%w_{BP/S}$	$M_c$	$\%(w/w)_{BP}$	$\frac{V_{BP\ sol.}}{V_v^{min}}$	Manufacturing Compaction Regime
	$\%w_{Soil}$	$\%w_{BP}$	$\%w_{water}$					
Mix 1	77.3%	6.2%	16.5%	8.0%	21.3%	29%	0.93	Single 10 MPa
Mix 2	78%	5.4%	16%	6.9%	20.8%	26%	0.89	Single 10 MPa
Mix 3	78.2%	7.4%	14.4%	9.4%	18.4%	36%	0.87	Single 10 MPa
Mix 4	76.5%	9.0%	14.5%	11.7%	18.9%	40%	0.94	Single 10 MPa
Mix 5	75.7%	9.8%	14.5%	12.9%	19.2%	42%	0.98	Single 10 MPa
Mix 6	74.8%	10.6%	14.6%	14.2%	19.5%	44%	1.02	Single 10 MPa
Mix 7	74.3%	11.0%	14.6%	14.8%	19.7%	45%	1.05	Single 10 MPa
Mix 8	74.0%	11.4%	14.6%	15.5%	19.7%	46%	1.06	Single 10 MPa
Mix 9	73.5%	11.9%	14.6%	16.1%	19.9%	47%	1.08	Single 10 MPa
Mix 10	73.1%	12.3%	14.7%	16.8%	20.1%	48%	1.11	Single 10 MPa
Mix 11	72.3%	13.1%	14.7%	18.1%	20.3%	50%	1.15	Single 10 MPa
Mix 12	71.3%	13.9%	14.8%	19.4%	20.7%	51%	1.20	Single 10 MPa
Mix 13	68.5%	13.3%	18.2%	19.5%	26.5%	45%	1.40	Single 10 MPa
Mix 14	74.7%	12.0%	13.2%	16.1%	17.6%	48%	1.01	Double 5 MPa
Mix 15	82.8%	7.0%	10.2%	8.4%	12.4%	40%	0.64	Double 5 MPa
Mix 16	84.6%	7.1%	8.3%	8.4%	9.8%	46%	0.55	Double 5 MPa
Mix 17	79.7%	9.2%	11.1%	11.6%	13.9%	45%	0.77	Double 5 MPa
Mix 18	77.6%	10.1%	12.3%	13.0%	15.8%	45%	0.87	Double 5 MPa
Mix 19	76.0%	10.6%	13.4%	14.9%	17.7%	44%	0.96	Double 5 MPa
Mix 20	75.6%	11.3%	13.0%	15.0%	17.2%	47%	0.97	Double 5 MPa

the lab to be around 4%. This value was used in subsequent mass ratio calculations. Reverse osmosis purified water with a resistance of 18.2 MΩ·cm was added to dry mixtures of aggregate and protein.

The mixture design methodology shown in Tab. 2 and Fig. 2 was used to create 20 mix designs presented in Tab. 3. Mixes 1 through 6 were designed so that  $V_{BP\ Sol.}$  was less than  $V_v^{min}$ . Mixes and, were designed to have the same biopolymer to soil mass ratio  $\%w_{BP/S}$ , but differing moisture content. Mix 3 to Mix 12 were designed to have the same water ratio  $\%w_{water}$ . Mixes 14 through 20 were manufactured using an enhanced compaction regimen to produce a higher and more uniform dry bulk density throughout the sample (Single 10 MPa compaction regime vs. Double 5 MPa compaction regime discussed in Section 3.2). Mix 14 was designed according to Tab. 1 for peak compressive strength at a biopolymer solution concentration  $\%(w/w)_{BP}$  of 48%.

### 3.2 Sample Manufacturing

BSC experimental samples were manufactured using a dry-mixing method, wherein dry, pre-weighed amounts of sand and protein were mixed before adding water using a silicone spatula. A total of six samples were created out of each mix. Mixture and specimen masses were measured using a Fischer Scientific A-250 laboratory balance accurate to ±10 mg. Finally, the mixtures of biopolymer, sand, and water were blended with a KitchenAid Stand Mixer for ten minutes until uniform.

A custom molding apparatus, consisting of a cylindrical mold with a 13 mm inner diameter and 76 mm height made from 316 stainless steel, was used to form the cylindrical BSC samples. A matching piston with a 12.8 mm diameter and 84 mm height was used to compact the samples. Freshly mixed BSC material was loaded into the cylinder and compacted, allowing for a specimen height-to-diameter ratio of 2:1. As shown in [Tab. 3](#), two compaction regimes were used. The “Single 10 MPa” compaction regime used an MTS Criterion Model 43 electromechanical universal testing machine to compact mixtures once under a pressure of 10 MPa. The “Double 5 MPa” compaction regime compacted the sample under a pressure of 5 MPa, prior to inverting the mold 180° (end over end) and compacting the specimen once again under a pressure of 5 MPa. After compaction, specimens were extruded from the mold, weighed, and placed in a Fisher Scientific IsoTemp Oven at 60°C for 24 hours to completely desiccate.

Once fully desiccated, each specimen’s top and bottom surfaces were cut parallel using a dry tile saw. Specimen diameter and height dimensions were measured using digital calipers accurate to  $\pm 0.05$  mm, using an average value of no less than 3 measurements. Dry mass measurements were also taken and used in conjunction with the caliper measurements to calculate desiccated specimen density.

### 3.3 Sample Testing

Unconfined uniaxial compression testing of BSC samples was conducted using an MTS Criterion Model 43 electromechanical universal testing machine (model number 50-292-603) and a 30 kN load cell. Digital axial displacement measurements were taken from the extension of the testing machine crossbar. Samples were loaded at a rate of 0.02 mm/s. Ultimate compressive strength ( $\sigma_c$ ) was taken as the peak load divided by the measured average cross-sectional area of the cylindrical specimen prior to testing. BSC specimens with large variations ( $\pm 0.2$  mm) in diameter throughout their height, or specimens with surfaces that did not make flat contact with the compression test platens, were excluded from the dataset.

Shrinkage caused by desiccation was measured photographically, for Mixtures 3, 5, 6, 9 and 12 ([Tab. 3](#)). Digital images were obtained using a Canon 70D DSLR camera, mounted on a tripod, with a 18–135 mm telephoto lens. To determine specimen shrinkage, a photo was taken of fresh specimens immediately after they had been compression molded and placed in the laboratory oven. These specimens were positioned on their sides in a v-shaped holder to ensure a clear image. An optical scale was placed adjacent to the specimen to facilitate measurements from the digital images. The specimens were desiccated over a period of 24 hours at 60°C. The relative change in mass of each specimen was verified to ensure complete desiccation through comparison to the mix design, and a final photo was taken of the desiccated specimens. Measurements of specimen height were observed from the digital images along the top-, middle-, and bottom-most locations of the sample using the image analysis software package FIJI [36]. Similarly, measurements of specimen width were taken along the left-, middle, and right-most locations. Drying shrinkage calculations were determined by measuring the average change in dimensions between the fresh and desiccated states, divided by the average dimensional value in the fresh state.

## 4 Experimental Results

The results of compressive strength tests and density measurements are shown in [Tab. 4](#) and shown graphically in [Fig. 3](#). The bulk densities were calculated using [Eqs. \(9\)](#) and [\(10\)](#) with the inputs being the biopolymer to soil ratio,  $\%w_{BP/S}$ , the moisture content,  $M_c$ , and the fresh and dry densities of BSC, measured experimentally.

$$\rho_{fresh, soil\ bulk} = \rho_{fresh, BSC} \times \frac{1}{1 + \%w_{BP/S} + M_c} \quad (9)$$

**Table 4:** Biopolymer-bound soil composite material characteristics and properties

Mix Name	Biopolymer Soil Ratio $\%W_{BP/S}$	Moisture Content $M_c$	Saturation Ratio $\frac{V_{BP\ sol.}}{V_v^{min}}$	Fresh Density $\rho_{fresh, BSC}$ (g/cm <sup>3</sup> )	Fresh Bulk Soil Density $\rho_{fresh, bulk\ soil}$ (g/cm <sup>3</sup> )	Dry Density $\rho_{dry, BSC}$ (g/cm <sup>3</sup> )	Dry Bulk Soil Density $\rho_{dry, bulk\ soil}$ (g/cm <sup>3</sup> )	Compressive Strength $\sigma_c$ (MPa)
Mix 1	8.0%	21.3%	0.94	1.66 ± 0.04	1.28	1.33 ± 0.05	1.23	4.2 ± 0.4
Mix 2	6.9%	20.8%	0.89	1.60 ± 0.02	1.25	1.34 ± 0.02	1.25	3.8 ± 0.6
Mix 3	9.4%	18.4%	0.87	1.73 ± 0.03	1.35	1.41 ± 0.02	1.28	6.5 ± 1.3
Mix 4	11.7%	18.9%	0.95	1.79 ± 0.03	1.37	1.48 ± 0.03	1.32	7.8 ± 0.9
Mix 5	12.9%	19.2%	0.99	1.84 ± 0.02	1.39	1.55 ± 0.02	1.36	9.8 ± 1.1
Mix 6	14.2%	19.5%	1.03	1.87 ± 0.01	1.40	1.59 ± 0.02	1.38	11.3 ± 1.1
Mix 7	14.8%	19.7%	1.05	1.86 ± 0.02	1.38	1.60 ± 0.02	1.38	10.0 ± 0.9
Mix 8	15.5%	19.7%	1.07	1.87 ± 0.01	1.38	1.61 ± 0.02	1.38	10.3 ± 0.4
Mix 9	16.1%	19.9%	1.09	1.88 ± 0.02	1.38	1.64 ± 0.02	1.40	9.9 ± 0.5
Mix 10	16.8%	20.1%	1.11	1.86 ± 0.03	1.36	1.59 ± 0.02	1.35	8.2 ± 0.5
Mix 11	18.1%	20.3%	1.16	1.86 ± 0.03	1.34	1.59 ± 0.02	1.34	7.2 ± 1.0
Mix 12	19.4%	20.7%	1.20	1.87 ± 0.01	1.33	1.58 ± 0.02	1.31	6.9 ± 0.4
Mix 13	19.5%	26.5%	1.40	1.87 ± 0.02	1.28	1.43 ± 0.02	1.19	3.6 ± 0.3
Mix 14	16.1%	17.7%	1.01	1.99 ± 0.01	1.45	1.74 ± 0.01	1.48	22.7 ± 0.4
Mix 15	8.4%	12.4%	0.64	1.72 ± 0.03	1.42	1.55 ± 0.01	1.43	10.0 ± 0.8
Mix 16	8.4%	9.8%	0.55	1.66 ± 0.02	1.41	1.53 ± 0.01	1.41	8.2 ± 0.9
Mix 17	11.6%	13.9%	0.77	1.83 ± 0.01	1.45	1.64 ± 0.00	1.47	16.6 ± 0.5
Mix 18	13.0%	15.8%	0.87	1.87 ± 0.01	1.45	1.67 ± 0.01	1.47	17.0 ± 0.4
Mix 19	14.0%	17.7%	0.96	1.92 ± 0.01	1.46	1.72 ± 0.01	1.51	21.9 ± 0.6
Mix 20	15.0%	17.2%	0.97	1.93 ± 0.00	1.46	1.71 ± 0.01	1.49	20.3 ± 0.7

$$\rho_{dry, soil\ bulk} = \rho_{dry, BSC} \times \frac{1}{1 + \%W_{BP/S}} \quad (10)$$

To understand the relationship between mixture variables (i.e., void saturation ratio, moisture content, and biopolymer to soil ratio) and BSC material properties, these mixture variables are plotted against the composite compressive strength (Figs. 3(a) through 3(c), respectively) and dry bulk density (Figs. 3(d) through 3(f), respectively). For comparison, data coming from mixes manufactured using different manufacturing protocols are plotted separately (Mixes 1–13 versus Mixes 14–20). As seen in Fig. 3(a), BSC materials exhibit a maximum compressive strength at void saturation ratios equal to approximately unity. When comparing Figs. 3(a) and 3(d), the strong correlation between dry bulk density and compressive strength becomes apparent, with the dry bulk density and compressive strength exhibiting the same trend as a function of void saturation ratio. As seen in Figs. 3(e) and 3(b), respectively, BSC materials exhibit a Proctor-like behavior with BSC maximum dry bulk density (and maximum compressive strength) being achieved at moisture content of approximately 19%. As seen in Figs. 3(c) and 3(f), the use of too much biopolymer can decrease the bulk density (and associated compressive strength even though there is more binder) with peak dry bulk density obtained at a biopolymer to soil ratio of approximately 17%. While the surface chemistries and physics that lead to this phenomenon are

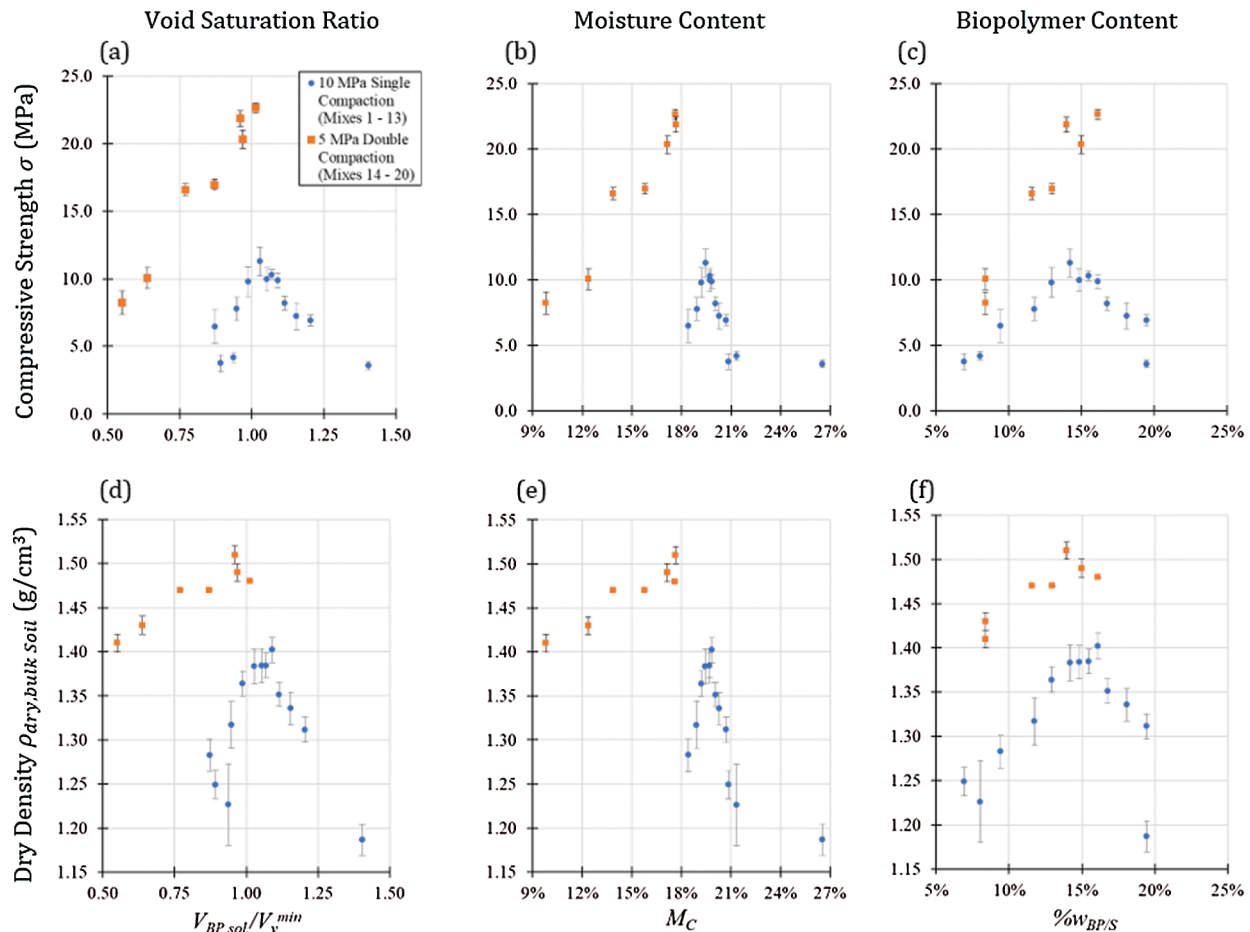


**Figure 3:** Biologically-bound soil composite (BSC) compressive strength versus (a) void saturation ratio, (b) moisture content, (c) biopolymer to soil ratio, and BSC dry bulk density vs. (d) void saturation ratio, (e) moisture content, and (f) biopolymer to soil ratio

outside of the scope of this study, further research should be done to isolate the chemical and physical interactions between the particles and binder at the interface and the effect on compressive strength.

To better illustrate the strong correlation between dry bulk density and compressive strength of BSC, the material's compressive strength is plotted against the soil dry bulk density and the BSC dry density in Figs. 4(a) and 4(b), respectively. As seen, the material's compressive strength is heavily dependent upon either of these measures. Soil dry bulk density was chosen as a key measure since it dissociates the data from the amount of biopolymer in the mix.

Drying shrinkage measurements, shown in Fig. 5, indicate that increasing amounts of biopolymer-water solution lead to higher drying shrinkage strains during desiccation, and potential residual stresses and internal damage. Unsurprisingly, drying shrinkage increases rapidly at biopolymer solution amounts that exceed a biopolymer saturation ratio equal to unity. This phenomenon results from all the voids between particles being filled and exhibiting an excess of liquid biopolymer solution. Thus, to achieve a maximum compressive strength for BSC materials, a void saturation ratio less than unity is recommended to limit material damage during the desiccation process.

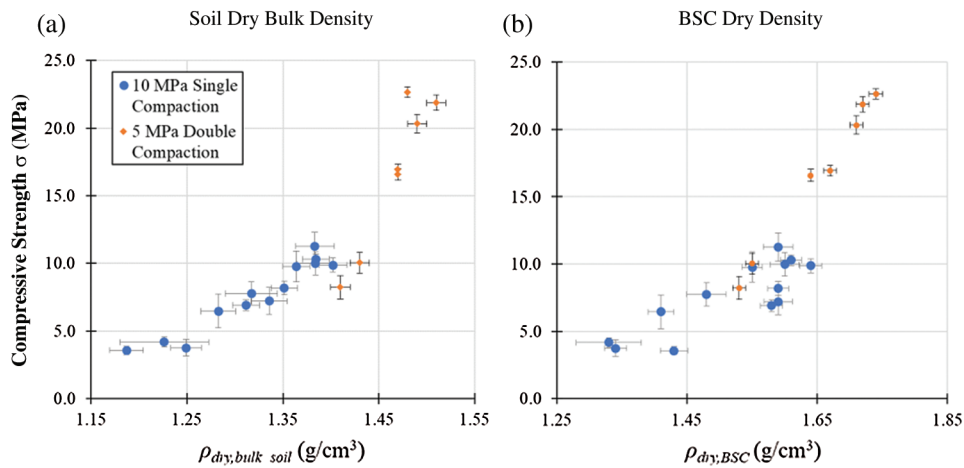


**Figure 4:** Biopolymer-bound soil composite (BSC) compressive strength vs. (a) particle dry bulk density, and (b) composite dry density

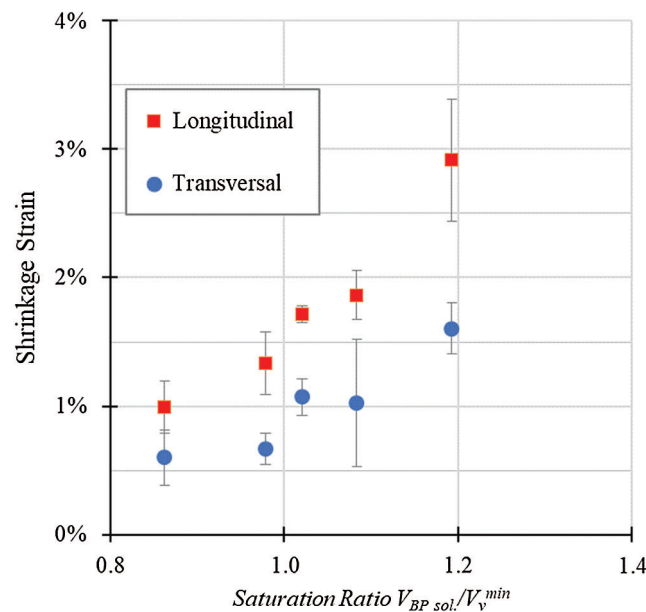


**Figure 5:** Shrinkage strain of fully desiccated BSC vs. void saturation ratio

## 5 Designing BSC Materials for Desired Compressive Strength

While the mixture design methodology presented in Tab. 2 can be used to design BSC for peak compressive strength, it does not enable design for a desired, or targeted, peak compressive strength (i.e., BSC with a desired compressive strength of 15 MPa). This would be analogous to designing ordinary Portland cement concrete mixtures for minimum water to cement ratio, but without knowing the long-standing relationship between  $w/c$  and compressive strength to facilitate rational concrete material design. Therefore, a basic relationship between mixture design parameters and compressive strength is needed.

As seen in Fig. 4, there exists a strong correlation between BSC peak compressive strength and dry soil bulk density. Fig. 3(c) shows that the biopolymer to soil ratio,  $\%w_{BP/S}$ , is also correlated with BSC peak compressive strength. Therefore, to facilitate BSC material design for desired peak compressive strength,

two linear models (one univariate and one bivariate) were fitted to relate peak compressive strength to dry soil bulk density and biopolymer to soil ratio presented in Eqs. (11) and (12)

*Bivariate Model:*

$$\sigma_c = a \times \rho_{dry,bulk\ soil} + b \times \%w_{BP/S} + c \tag{11}$$

$$a = 44.3 \quad b = 86.6 \quad c = -59.5$$

*Univariate Model:*

$$\sigma_c = a \times \rho_{dry,bulk\ soil} + c \tag{12}$$

$$a = 62.7 \quad c = -75.0$$

Experimental data from Mixes 7 to 13 (in which the biopolymer saturation ratio is above unity) were removed since these mix designs are not within the “efficient and feasible” mixture design space shown in Fig. 2. The bivariate and univariate models have R-squared values of 0.924 and 0.826, respectively, and capture the effect of biopolymer to soil ratio  $\%w_{BP/S}$  and dry bulk soil density  $\rho_{dry,bulk\ soil}$  on compressive strength  $\sigma_c$  observed in the experimental data (Fig. 6).

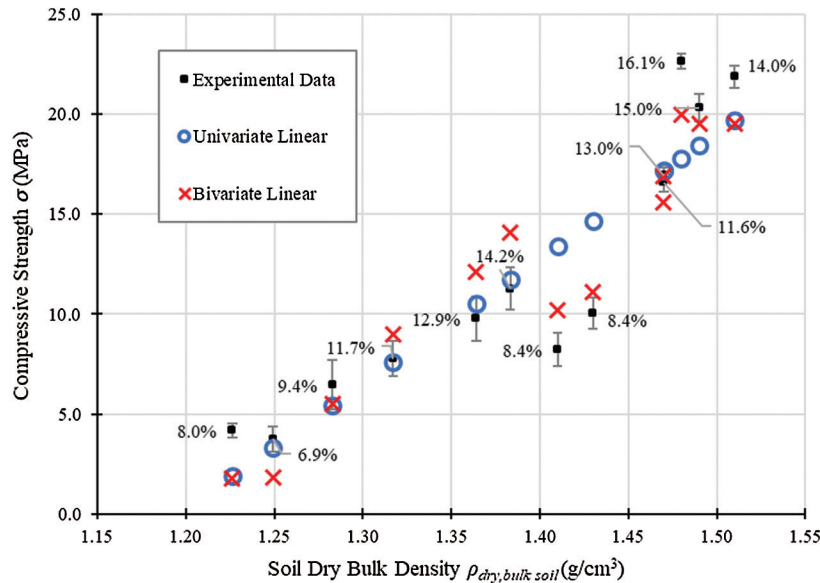


**Figure 6:** Compressive strength vs. dry bulk density for “efficient and feasible” BSC mixture designs. Data labels provide the biopolymer to soil ratio  $\%w_{(BP/S)}$  of each mix. Standard deviation of the experimental results of the compressive strength of the mix are represented by the error bars

## 6 Discussion

From Fig. 6, it can be observed that the model for determining peak compressive strength corroborates the design theory and methodology presented, wherein ultimate compressive strength increases with both biopolymer content and dry bulk density, both of which have positive coefficients in the bivariate and univariate models. Thus, to obtain peak compressive strength for BSC materials, the material designer should look to (i) increase the soil dry bulk density  $\rho_{dry,bulk\ soil}$  and (ii) increase the biopolymer to soil ratio  $\%w_{BP/S}$ , while (iii) not exceeding a biopolymer saturation ratio,  $V_{BP\ Sol.}/V_v^{min}$  of unity. Combining the BSC design space shown in Fig. 2 and the bivariate linear model of peak compressive strength in

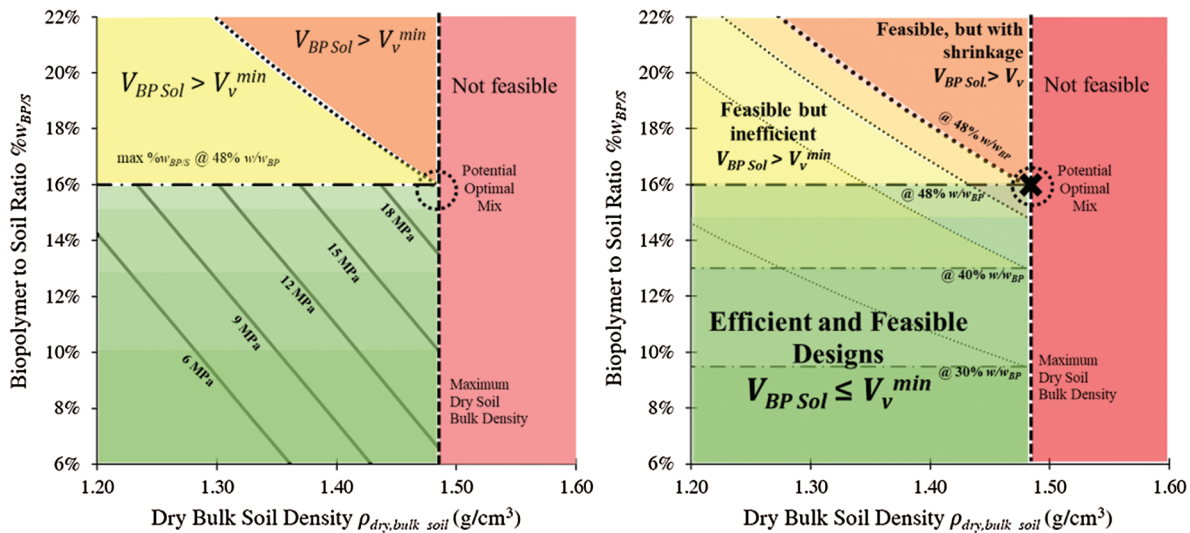


**Figure 7:** (a) Design guide for achieving targeted ultimate compressive strength of BSC materials manufactured using AP920 biopolymer and #90 grade sand, and (b) variation of the design space as a function of practically achievable biopolymer concentration  $\% (w/w)_{BP}$

Eq. (11), a specific mixture design guide can be created and is shown in Fig. 7(a) for the BSC material comprised of grade #90 sand and AP920 biopolymer. Analogous to the seminal figure relating water-to-cement ratio and compressive strength for Portland cement concrete, a BSC material designer can use a design guide, such as Fig. 7(a), to design a BSC mixture for a desired peak compressive strength by selecting a biopolymer to soil and associated dry bulk density of the BSC soil. Since manufacturing techniques can limit the amount of biopolymer solution concentration able to be incorporated in the mix, Fig. 7(b) shows how the design space varies as a function of biopolymer concentration  $\% (w/w)_{BP}$ . For BSC materials using AP920 as a binder, the maximum biopolymer concentration that is practically workable is approximately 48%.

Although the models presented in Fig. 6, are empirical, they provide a better fit than the previously proposed model based on the sliding wingtip crack theory originally devised for rocks [15]. In the previous model, there was an overestimation of the compressive strength at both the low and high values of dry soil bulk density. On the current model, there is a slight underestimate of the strength at the edge values which is conservative thus preferred for material design. As computational models for BSC advance, the design tools proposed in this paper can be easily modified to incorporate new strength models in Fig. 7(a).

It is important to note that the proposed mixture design methodology shown in Tab. 2 does not yet fully consider optimum moisture content for compaction of the soil in BSC. As was shown by Proctor [30], soils have an optimum moisture content for compaction usually between 8–15% water content. Improved compaction, measured by changes in bulk density, increases the bearing strength of soils through enhanced packing of the particles and subsequent decreases in void volume and void size. Additionally, the optimum moisture content depends on the amount of compaction effort, with increased effort requiring less moisture for peak aggregate density. The effect of proctor phenomena and biopolymer concentration on BSC dry bulk density and peak compressive strength remains a focus of current efforts and future work.

The proposed methodology to produce strong biopolymer-bound soil composites could be potentially extended to other construction applications, such as soils treated with biopolymer binders for soil

improvement or brick manufacturing. **Tab. 1** shows a literature summary of recent work in soil-biopolymer composites highlighting the biopolymer and soil used, as well as the mix design by reporting moisture content  $M_c$ , biopolymer to soil ratio  $\%w_{BP/S}$  and resulting bulk density and compressive strength. Previous work has focused on polysaccharides (e.g., gums and starches) working as the biopolymer binder at low biopolymer to soil ratio  $\%w_{BP/S}$  (0.005–5%). At these low biopolymer to soil ratios, the resulting compressive strengths values ranged from 0.06 to 6.5 MPa. In contrast, the biopolymer-bound soil composite presented in this paper used proteins as the biopolymer binder at a high biopolymer to soil ratio to produce compressive strengths upwards 20 MPa. This may be due to the higher concentration of biopolymer solutions associated with BSC materials examined in this paper. Regardless, for BSCs to become viable construction materials, reliably achieving high compressive strength is crucial. The proposed methodology has the potential to do so with different biopolymer and soil combinations, although further research is needed when extrapolating to other biopolymers or fine grained soils, such as clay, due to the electrostatic interactions of between fine soil particles with powdered biopolymers [6].

## 7 Conclusions

This work experimentally investigated the mechanisms that lead to the development of peak compressive strength of Biopolymer-bound Soil Composites (BSC) by varying the amounts of biopolymer binder and water added to the mixture. The investigation led to a new methodology for designing mixtures of BSC for maximum compressive strength. In order to calculate the gravimetric amounts of aggregate, biopolymer, and water, the methodology requires the mixture designer to define the desired mixture volume, the target biopolymer to soil ratio, and knowing the maximum bulk density of the soil, ensure that the biopolymer saturation ratio does not exceed unity. The methodology was ultimately summarized in a materials design chart that allows for the rational design of BSC materials for peak compressive strength by varying the biopolymer to soil ratio and the dry bulk density of the soil used in BSC materials.

Compressive strength testing results compared to the dry bulk density of BSC samples revealed a linear relationship between these two material parameters Dry bulk density increases until the void saturation ratio exceeds unity, after which point it starts decreasing. Drying shrinkage test results show that increased shrinkage occurs when the volume of protein solution exceeds the minimum void volume during sample manufacture. The damage to biopolymer binding structure caused by shrinkage decreases composite binding and results in a state of pre-damage in the material. Both effects contribute to a decrease in BSC compressive strength with increasing biopolymer solution above a biopolymer saturation ratio of unity.

This work focused on the impact of the constituents and their effect on BSC peak compressive strength; further investigations are needed to delve into additional manufacturing variables, such as rate of desiccation and chemical denaturation of the biopolymers during manufacture. Furthermore, investigations into the optimum moisture content based on the Proctor method should be conducted to determine if a similar effect is found on peak BSC compressive strength.

**Acknowledgement:** The authors would like to thank the following individuals for their collaborative efforts in carrying out the research discussed in this paper: Ms. Natalie Ferrante and Ms. Evelyn Li for their contributions to the shrinkage and compressive strength studies. Additional thanks to Dr. Edward J. Garboczi from NIST (Boulder, CO) for his support in capturing  $\mu$ CT images of BSC materials.

**Funding Statement:** The authors would also like to acknowledge partial graduate student funding from the Charles H. Leavell Fellowship at Stanford University, along with partial graduate support from the NASA Ames Research Center Chief Technologist and NASA's Game Changing Development Program for H. Roedel; National Science Foundation Graduate Research Fellowship [Grant No. DGE-114747], Stanford Graduate Fellowship under the donation of William R. and Sara Hart Kimball and Stanford's DARE

Fellowship funding for I. Rosa and NASA's Space Technology Research Fellowship for M. Allende. Any opinions, findings, and conclusions or recommendations expressed in this material are those of the authors and do not necessarily reflect the views of the United States National Science Foundation. The authors would like to acknowledge the John A. Blume Earthquake Engineering Center at Stanford University and the Stanford Vice Provost for Undergraduate Education for laboratory equipment funding and undergraduate research funding, respectively.

**Availability of Data and Materials:** Any additional data not presented in this paper is available upon request to the corresponding author.

**Conflicts of Interest:** The authors declare that they have no conflicts of interest to report regarding the present study.

## References

1. Matos, G. R. (2017). *Use of raw materials in the United States from 1900 through 2014* (USGS Numbered Series No. 2017–3062). Reston, VA: US. Geological Survey, Department of the Interior. <https://doi.org/10.3133/fs20173062>.
2. US EPA. (2015). *Inventory of US. greenhouse gas emissions and sinks: 1990–2013* (No. EPA 430-R-15-004). Washington, D.C.: United States Environmental Protection Agency. <https://www.epa.gov/ghgemissions/inventory-us-greenhouse-gas-emissions-and-sinks-1990-2013>.
3. The White House. (2010). *National space policy of the United States of America*. [https://obamawhitehouse.archives.gov/sites/default/files/national\\_space\\_policy\\_6-28-10.pdf](https://obamawhitehouse.archives.gov/sites/default/files/national_space_policy_6-28-10.pdf).
4. Khatami, H. R., O'Kelly, B. C. (2013). Improving mechanical properties of sand using biopolymers. *Journal of Geotechnical and Geoenvironmental Engineering*, 139(8), 1402–1406. DOI 10.1061/(ASCE)GT.1943-5606.0000861.
5. Chang, I., Cho, G. C. (2014). Geotechnical behavior of a beta-1, 3/1, 6-glucan biopolymer-treated residual soil. *Geomechanics and Engineering*, 7(6), 633–647. DOI 10.12989/gae.2014.7.6.633.
6. Chang, I., Im, J., Prasadhi, A. K., Cho, G. C. (2015). Effects of Xanthan gum biopolymer on soil strengthening. *Construction and Building Materials*, 74, 65–72. DOI 10.1016/j.conbuildmat.2014.10.026.
7. Ayeldeen, M. K., Negm, A. M., El Sawwaf, M. A. (2016). Evaluating the physical characteristics of biopolymer/soil mixtures. *Arabian Journal of Geosciences*, 9(5), 371. DOI 10.1007/s12517-016-2366-1.
8. Qureshi, M. U., Chang, I., Al-Sadarani, K. (2017). Strength and durability characteristics of biopolymer-treated desert sand. *Geomechanics and Engineering*, 12(5), 785–801. DOI 10.12989/gae.2017.12.5.785.
9. Dove, C. A., Bradley, F. F., Patwardhan, S. V. (2016). Seaweed biopolymers as additives for unfired clay bricks. *Materials and Structures*, 49(11), 4463–4482. DOI 10.1617/s11527-016-0801-0.
10. Chang, I., Jeon, M., Cho, G. C. (2015). Application of microbial biopolymers as an alternative construction binder for earth buildings in underdeveloped countries. *International Journal of Polymer Science*, 2015(3), 1–9. DOI 10.1155/2015/326745.
11. Muguda, S., Booth, S. J., Hughes, P. N., Augarde, C. E., Perlot, C. et al. (2017). Mechanical properties of biopolymer-stabilised soil-based construction materials. *Géotechnique Letters*, 7(4), 309–314. DOI 10.1680/jgele.17.00081.
12. Brownsey, G. J., Noel, T. R., Parker, R., Ring, S. G. (2003). The glass transition behavior of the globular protein bovine serum albumin. *Biophysical Journal*, 85(6), 3943–3950. DOI 10.1016/S0006-3495(03)74808-5.
13. Roedel, H., Lepech, M. D., Loftus, D. J. (2014). Protein-Regolith composites for space construction. *Proceedings of the 14th ASCE International Conference on Engineering, Science, Construction and Operations in Challenging Environments. Presented at the Earth and Space 2014: Engineering for Extreme Environments, St. Louis, MO: ASCE Publications*. <http://ascelibrary.org/doi/pdfplus/10.1061/9780784479179.033>.
14. Rosa, I., Roedel, H., Lepech, M., Loftus, D., Garboczi, E. (2016). Three-phase statistically equivalent periodic unit cells for protein-bound soils. *Proceedings of the 15th ASCE International Conference on Engineering, Science, Construction and Operations in Challenging Environments. Presented at the ASCE Earth and Space 2016: Engineering for Extreme Environments, Orlando, FL: ASCE Publications*. <https://doi.org/10.1061/9780784479971.072>,

15. Roedel, H., Rosa, I., Allende, M. I., Lepech, M. D., Loftus, D. J. et al. (2019). Prediction of ultimate compressive strength for biopolymer-bound soil composites (BSC) using sliding wingtip crack analysis. *Engineering Fracture Mechanics*, 218, 106570. DOI 10.1016/j.engfracmech.2019.106570.
16. Kosmatka, S. H., Kerkhoff, B., Panarese, W. C. (2011). *Design and control of concrete mixtures*. Portland Cement Association, Skokie, Illinois USA.
17. Huber, G. (2013). History of asphalt mix design in North America, Part II: Superpave. *Asphalt*, 28(2). <http://asphaltmagazine.com/history-of-asphalt-mix-design-in-north-america-part-2/>.
18. Miller, S. A., Monteiro, P. J. M., Ostertag, C. P., Horvath, A. (2016). Comparison indices for design and proportioning of concrete mixtures taking environmental impacts into account. *Cement and Concrete Composites*, 68, 131–143. DOI 10.1016/j.cemconcomp.2016.02.002.
19. Živica, V. (2009). Effects of the very low water/cement ratio. *Construction and Building Materials*, 23(12), 3579–3582. DOI 10.1016/j.conbuildmat.2009.03.014.
20. McLeod, N. W. (1956). Relationships between density, bitumen content, and voids properties of compacted bituminous paving mixtures. *Highway Research Board Proceedings, Washington, D.C. USA*, 35. <https://trid.trb.org/view/101296>.
21. Asphalt Institute. (1996). *Superpave mix design*. Lexington, KY: Asphalt Institute.
22. Quiroga, P. N., Fowler, D. W. (2003). *The effects of the aggregates characteristics on the performance of Portland Cement Concrete (No. Research Report ICAR 104-1F)* (p. 382). Austin, TX: University of Texas.
23. Roedel, H. (2017). *On the compressive strength and sustainability of protein bound concretes*. Stanford University, Stanford, CA. <https://searchworks.stanford.edu/view/12082110>.
24. Bernhardt, J., Pauly, H. (1980). Pycnometric vs. densimetric measurements of highly viscous protein solutions. *Journal of Physical Chemistry*, 84(2), 158–162. DOI 10.1021/j100439a007.
25. Durchschlag, H. (1989). Determination of the partial specific volume of conjugated proteins. *Colloid and Polymer Science*, 267(12), 1139–1150. DOI 10.1007/BF01496937.
26. Vavrik, W. R., Pine, W. J., Carpenter, S. H. (2002). Aggregate blending for asphalt mix design: bailey method. *Transportation Research Record*, 1789(1), 146–153. DOI 10.3141/1789-16.
27. Shen, S., Yu, H. (2011). Characterize packing of aggregate particles for paving materials: particle size impact. *Construction and Building Materials*, 25(3), 1362–1368. DOI 10.1016/j.conbuildmat.2010.09.008.
28. de Larrard, F., Sedran, T. (1994). Optimization of ultra-high-performance concrete by the use of a packing model. *Cement and Concrete Research*, 24(6), 997–1009. DOI 10.1016/0008-8846(94)90022-1.
29. Sobolev, K., Amirjanov, A. (2010). Application of genetic algorithm for modeling of dense packing of concrete aggregates. *Construction and Building Materials*, 24(8), 1449–1455. DOI 10.1016/j.conbuildmat.2010.01.010.
30. Proctor, R. (1933). Fundamental principles of soil compaction. *Engineering News-Record*, 111(13). [https://link.springer.com/referenceworkentry/10.1007%2F978-3-319-12127-7\\_62-1](https://link.springer.com/referenceworkentry/10.1007%2F978-3-319-12127-7_62-1).
31. ASTM International. (2017). ASTM C29/C29M-17a standard test method for bulk density (“Unit Weight”) and voids in aggregate. *ASTM*. [https://doi.org/10.1520/c0029\\_c0029m-17a](https://doi.org/10.1520/c0029_c0029m-17a).
32. P. W. Gillibrand Co., Inc. (2015). Specialty sands & construction products. *P. W. Gillibrand Co., Inc. - Construction Products*. Retrieved April 17, 2018. <https://www.pwgillibrand.com/simi-valley-sand-location>.
33. Roedel, H., Rosa Plata, I., Lepech, M., Loftus, D. (2015). Sustainability assessment of protein-soil composite materials for limited resource environments. *Journal of Renewable Materials*, 3(3), 183–194. DOI 10.7569/JRM.2015.634107.
34. APC Inc. (2015, September). AP920(R) Animal plasma. <http://robinsonbioproducts.com/wp-content/uploads/2015/09/AP920-Bovine-SPEC.pdf>.
35. Dàvila, E., Parés, D., Cuvelier, G., Relkin, P. (2007). Heat-induced gelation of porcine blood plasma proteins as affected by pH. *Meat Science*, 76(2), 216–225. DOI 10.1016/j.meatsci.2006.11.002.
36. Schindelin, J., Arganda-Carreras, I., Frise, E., Kaynig, V., Longair, M. et al. (2012). Fiji: an open-source platform for biological-image analysis. *Nature Methods*, 9(7), 676–682. DOI 10.1038/nmeth.2019.